INTERNATIONAL JOURNAL OF OPTIMIZATION IN CIVIL ENGINEERING
Int. J. Optim. Civil Eng., 2018; 8(4):525-545

PERFORMANCE-BASED SEISMIC DESIGN OPTIMIZATION FOR MULI-COLUMN RC BRIDGE PIERS, CONSIDERING QUASI-ISOLATION

H. Fazli[*, †] and A. Pakbaz
Department of Civil Engineering, Payame Noor University, Tehran, Iran

ABSTRACT

In this paper an optimization framework is presented for automated performance-based seismic design of bridges consisting of multi-column RC pier substructures. The beneficial effects of fusing components on seismic performance of the quasi-isolated system is duly addressed in analysis and design. The proposed method is based on a two-step structural analysis consisting of a linear modal dynamic demand analysis and a nonlinear static capacity evaluation of the entire bridge structure. Results indicate that the proposed optimization method is capable of producing cost-effective design solutions combining the fusing behavior of bearings and yielding mechanism of piers. The optimal designs obtained from models addressing the performance of fusing components are far more efficient than those that do not take care of quasi-isolation behavior.

Keywords: optimization; performance-based seismic design; bridge; quasi-isolation; MCBO.

Received: 20 October 2017; Accepted: 15 January 2018

1. INTRODUCTION

Performance based seismic design (PBSD) is a process in which performance requirements are translated and integrated into design. Using PBSD, structures can be designed to particular damage levels for different earthquake motions. PBSD formulated as a structural optimization problem is a topic of growing interest and has been the subject of extensive research over the last years. A number of studies have been published in the past where the concept of performance-based design optimization was applied to different structures including steel structures [1-4], reinforced concrete structures [5] and bridge piers [6-8].

Bridges are essential lifelines for communities and their performance during a moderate

[*]Corresponding author: Department of Civil Engineering, Payame Noor University, Tehran, Iran
[†]E-mail address: hfazli@alumni.iust.ac.ir (H. Fazli)

to high seismic event is of great importance. Transition to performance based design of bridges is happening quickly since many design guidelines have adopted PBSD methodology (CSA, 2014 [9]; FHWA-NHI, 2014 [10]). Performance based design of bridges was investigated by some researchers including Mackie & Stojadinović [11], Priestley [12], Dawood & ElGawady [13] and Floren & Mohammadi [14]. A comprehensive study from U.S. National Cooperative Highway Research Program [15] presented a summary and guideline for performance based seismic design of bridges.

In order to achieve the performance goals for seismic design of bridges, several global design strategies have been proposed. A common bridge design strategy employed in high seismic regions is to design the substructure and superstructure to remain elastic while a fusing mechanism is implemented at the interface between the two. An extension of this design strategy is the earthquake resisting system (ERS) developed by the Illinois DOT (IDOT) [16] which is named quasi-isolated bridge design. The basic idea is that typical bearings can be designed and detailed such that they act as fuses, to limit the forces transmitted from the superstructure to the substructure. The configuration and design approach of a quasi-isolated system is significantly simplified and its construction cost is considerably reduced relative to a classically isolated system. The results of extensive research on global seismic performance of prototype bridges ([17-19]) indicate that quasi-isolation may provide adequate seismic performance by limiting forces transmitted to substructure and increasing the displacement capacity of the system, provided that some calibration of fusing component capacities (i.e. retainers and fixed bearings) is undertaken.

In this paper, an optimization approach is adopted to the performance-based seismic design of multi-column RC bridge piers exploiting the concept of quasi-isolation. A three-span continuous steel I-girder superstructure on multi-column pier substructures, typical of Illinois bridge configurations, is selected as a prototype for illustration. Two seismic hazard levels are considered with different performance criteria for each level. Design parameters to be optimized consist of column diameters, numbers and diameters of the longitudinal reinforcements, diameters and spacing of the transverse reinforcement and the fusing component capacities. The structural optimization seems to be the appropriate framework for finding the most efficient design in terms of cost and performance for such a highly nonlinear problem.

2. PERFORMANCE-BASED SEISMIC BRIDGE DESIGN

Performance-based seismic design (PBSD) is the modern conceptual approach to structural design, which is based on the principle that a structure should meet performance objectives for multiple seismic hazard levels, ranging from small magnitude earthquakes of a short return period, to more intensive events with long return periods. A performance objective is a combination of performance levels each linked to a specific hazard level. The performance level can be specified limits on any response parameter such as stresses, strains, displacements, accelerations, damage states or the failure probability [20, 21]. Various definitions and specifications of performance levels are introduced in the literature. According to FHWA *Seismic Retrofitting Manual*, 2006 [22], performance criteria for a typical concrete bridge are defined for four performance levels as per Table 1. This table

also presents the correlation of performance levels with damage states.

Table 1: Performance levels and corresponding damage states

Performance level	Damage state
Fully operational	Minor damage
Operational	Moderate damage
Life safety	Severe damage
Near collapse	Near collapse

The full PBSD process may be decomposed into the following four steps, as outlined by Moehle and Deierlein [23].

1. Seismic hazard analysis
2. Structural analysis
3. Damage analysis
4. Loss analysis

The first three steps are briefly discussed below.

Seismic hazard analysis is intended to quantify the seismic input at the site in terms of intensity measures (IM), such as spectral acceleration (SA). Two basic types of seismic hazard analysis (probabilistic and deterministic analysis) are commonly employed in design practice. In the probabilistic method which is the method of choice by AASHTO [24, 25], the uncertainties in the occurrence of earthquakes on any sources affecting a site are taken into account in the attenuation relationships. These relationships are then combined to form the probability of exceedance of a seismic hazard level or alternatively, the average return period for a given value of seismic hazard (e.g., ground acceleration or spectral acceleration). AASHTO in 2007 adopted a 1,000-year return period (approximately a 7% chance of exceedance in 75 years) as the basis for design for ordinary or conventional bridges, with essentially a 'no-collapse' design philosophy which implies a 'life-safety' performance. In the context of PBSD, more than one return period may be included, considering different performance in each event. For instance, NCHRP, 2001 [26] proposed two seismic hazard levels of a 'rare' earthquake with a 2,500-year return period (corresponding to 3% probability of exceedance in 75 years), and an 'expected' earthquake with a 100-year return period (corresponding to 50% probability of exceedance in 75 years). Two levels of performance are specified for ordinary bridges, namely 'life safety' under a 'rare' earthquake in which significant damage (but not loss of life) is expected and 'operational' performance under an 'expected' earthquake, with the bridge suffering minimal damage. The aforementioned seismic hazard levels are listed in Table 2.

Table 2: Proposed seismic hazard levels

Earthquake hazard level	Return period in years	Probability of exceedance
Expected earthquake	100	50% in 75 years
Design level earthquake	1000	7% in 75 years
Rare Earthquake	2500	3% in 75 years

Structural analysis relates the seismic input to structural response characterized by

engineering demand parameters (EDPs), such as strains, rotations, displacements, drifts, or internal forces. Various methods for structural analysis are developed, based on the explicit treatment of inelasticity and dynamic behavior. Many of the current PBSD procedures use a combination of analysis methods. For example, the *Guide Specifications for LRFD Seismic Bridge Design* (AASHTO SGS) [24] uses a linear dynamic analysis to determine seismic displacement demand of a bridge, while a nonlinear static pushover analysis is used to determine the displacement capacity of either the individual piers or the bridge as a whole.

Damage analysis relates the structural and nonstructural response (internal forces, deformations, accelerations, displacements, strains, curvatures, and rotations) to damage measures (DMs). Finally, the DMs can be related to the functionality or loss of the bridge in terms of performance levels, such as: Fully Operational, Operational, Life Safety, and Collapse. Damage sustained by a structure (and its nonstructural components) is directly relatable to the use or loss of a system after an earthquake. Thus it is fundamental to the PBSD methodology to determine the type of damage and the likelihood that such damage will occur in particular components of the structural system.

In order to correlate engineering demand parameters (EDPs) with DMs, extensive laboratory experiments are conducted on bridge components, sub-assemblages, and systems. Relationships between damage and performance levels have also been developed which are based on the perceived risk and observed actual performance of components and structures in past earthquakes. These correlations have been defined within the literature, but there is often a disparity in what is reported between researchers, institutions, and organizations. An example of such a correlation, which is based on the five-level performance evaluation approach developed and used extensively by the University of California, San Diego [27] is presented in modified form in Table 3. Note that these correlations are presented as an example and may show large discrepancies with design procedures like Caltrans [28] or AASHTO [25].

It should be noted that the full PBSD performed at the highest level, is a probabilistic process which has to comprehensively consider the outcomes and uncertainties from seismic loading. However, due to the currently limited data and analytical tools, design methodologies are developed that permit the process to be implemented in deterministic fashion without full consideration of the uncertainties inherent at each step of the process. The current design provisions of either buildings or bridges, only relate the seismic input probabilistically, but not the remaining three steps. As an example, the current AASHTO SGS employs deterministic analysis where specific strain or displacement limits are considered for the performance of structural components.

Table 3: Bridge performance/Damage/Design parameters (Hose and Seible 1999 [27])

Performance Level	Damage Classification	Damage Description	Steel Strain	Concrete Strain	Drift (%)	Displacement Ductility
Fully operational	No	Onset of hairline cracks	<0.005	<0.0032	<1.0	<1.0
Operational	Minor	Crack widening /Theoretical first yield of longitudinal reinforcement	0.005	0.0032	1.0	1.0
Life safety	Major	Formation of very wide	0.019	0.01	3.0	2.0

Near collapse		cracks/ Extended concrete spalling	0.048	0.027	5.0	6.0
Collapse	Local failure/ collapse	Buckling of main reinforcement/ Rupture of transverse reinforcement/ Crushing of core concrete	0.063	0.036	8.7	8.0

The design methodology embedded into AASHTO SGS is a displacement-based method (DBM) which focuses the designer's attention on checking the system deformation capacity rather than selecting the precise resistance of the yielding or energy dissipating elements. Therefore, this method is better suited for extension into performance-based design. In the DBM, instead of calculating required internal forces in the structure, a trial design is checked against the displacement demand imposed by the seismic input. Thus, the designer simply proposes a lateral seismic resisting system and corresponding element strengths then checks to ensure that the displacement capacity is adequate. The method is based on the capacity design principles of AASHTO, in that locations for damage are selected; these locations then are detailed to deliver adequate displacement or ductility capacity, and that capacity is directly checked. In the DBM, the effect of confinement steel, for example, is directly included in the calculation of displacement capacity. Thus, the designer has some direct control over the amount of ductility or deformation capacity that will be provided versus the amount of ductility that is required.

The AASHTO SGS method could be converted to a nominally performance-based approach by using definable deformation response limits, such as concrete and reinforcing steel strains, member curvatures or rotations, member ductility demands or other EDPs that are correlated to specific damage states-for instance, spalling or bar buckling. Therefore, instead of assessing the displacement demand against the displacement capacity, a direct check of local member drift or ductility demands is made to ensure that the specified limits for the associated performance level are not exceeded. For instance, a life safety/no collapse performance criteria would require the bridge to provide a Full-Ductile Response. This requirement implies that the substructure members should ensure large ductility capacity, μ_C, such that ductility demands, μ_D, of up to 6.0 for multi-column piers are accomodated. The operational performance, on the other hand, would imply a Limited-Ductility response and the requirement on the ductility demands is reduced ($\mu_D \leq 2.0$).

3. QUASI-ISOLATION OF BRIDGES

Seismic isolation is a well-established design philosophy which is employed in bridge engineering to provide earthquake resistance in high seismic regions. However, due to design complexities and higher cost of isolation systems, a more economical and pragmatic design philosophy known as Quasi-isolation is preferred in regions of moderate seismic hazard. In this design methodology, typical bridge bearings are employed as fuses to limit seismic forces transmitted to the substructure. Extensive research is carried out to investigate the seismic performance of quasi-isolated systems, mainly consisting of elastomeric

bearings, i.e. IDOT Type I and Type II bearings, and the low-profile fixed bearings.

IDOT Type I bearings are steel-reinforced elastomeric bearings directly placed on the concrete substructure (vulcanized to only a top steel plate) (Fig. 1a, 1b). IDOT Type II bearings consist of a steel-reinforced elastomeric bearing vulcanized to steel plates on both sides. The bottom steel plate is connected to the substructure via anchor bolts. The middle plate is coated on the top side with poly-tetra-fluoro-ethylene (PTFE). Another top plate with a stainless steel mating surface carries the girder load directly onto the PTFE surface (Fig. 1c). Elastomeric bearings permit thermal expansion in the longitudinal direction of the bridge, however the bridge movement is restricted in the transverse direction by using L-shaped steel side retainers. Low-profile fixed bearings consist of a bottom plate anchored to the substructure that mates with a curved top plate attached to the superstructure (Fig. 1d). Two pintles are provided to carry traffic braking loads and prevent global service load movement of the structure. The quasi-isolated system proposed by IDOT employs a set of fixed bearings at one intermediate substructure, and all other substructures are instrumented with elastomeric bearings. Low-profile fixed bearings together with retainer components are intended to break-off and permit sliding at high earthquake loads.

The results of extensive research indicate that quasi-isolated bridges especially those with Type I bearings exhibit reliable seismic behavior and prevent system collapse. These results also suggest that seismic performance may be improved by calibrating fuse component capacities i.e. selecting smaller anchor bolt diameters for retainers and low-profile fixed bearings.

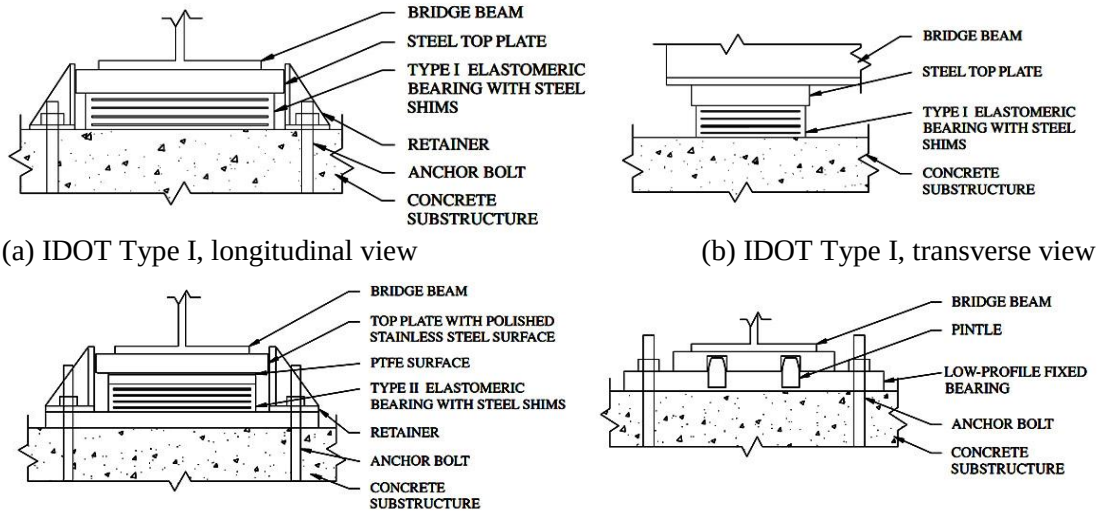

(a) IDOT Type I, longitudinal view (b) IDOT Type I, transverse view

(c) IDOT Type II, longitudinal view (d) Low-profile fixed, longitudinal view

Figure 1. Bridge bearing types under consideration [29]

4. IMPLEMENTATION OF PERFORMANCE-BASED SEISMIC DESIGN OPTIMIZATION FOR QUASI-ISOLATED BRIDGES

The present paper aims at using the Modified Colliding Bodies Optimization (MCBO)

algorithm to solve the optimization problem for the PBSD of quasi-isolated bridge systems with RC multi-column pier substructures. In order to implement the algorithm, a three-span bridge with concrete girder superstructure on multi-column pier substructures is selected as a prototype for illustration (see Fig. 2 for a schematic of this prototype bridge). Low-profile fixed bearings are installed at one of the intermediate piers (pier 2), while Type I IDOT elastomeric bearings are used at the other pier and abutment locations. This paper is focused on optimal design of bridge piers and fusing components such that the desired performance of overall bridge system under various seismic hazard levels is realized. The required parameters for performance-based design optimization are discussed in the following subsections. Finally based on the proposed procedure, several feasible design solutions for pier and fusing components are obtained. In order to provide a basis for comparison of optimal designs between the systems with and without quasi-isolation, the optimization process is also implemented on conventional bridge systems excluding the fuse components.

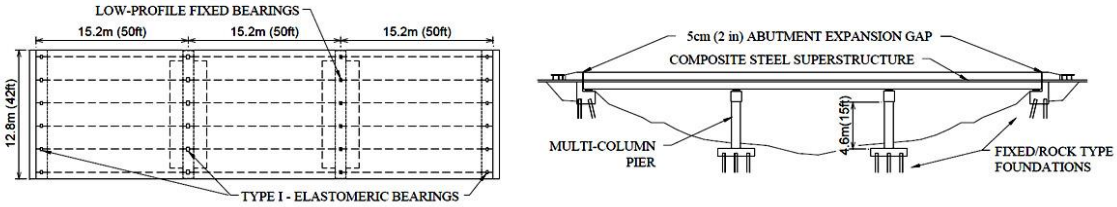

Figure 2. Quasi-isolated bridge prototype

4.1 Design variables

The optimization is carried out for 8 design variables including: IDOT I elastomeric bearings dimensions, retainer sizes for IDOT bearing, Fixed-bearing model (consisting of pintles and anchor bolt diameters), diameter of pier columns D (mm), and the number of longitudinal reinforcements *n*, the diameter of the longitudinal reinforcement D_L (mm), the diameter of the transverse reinforcement D_T (mm) and the spacing of the transverse reinforcement *m* (mm). Design variables are tabulated in Table 4.

Table 4: Design variables and explicit constraints

Design variables	**Constraints**
Circular Columns diameter (D)	80-150 cm
Diameter of the longitudinal reinforcement D_L	16,18,20,22, 24,25,26,28, 30,32,34,36,38 mm
Diameter of the transverse reinforcement D_T	8,10,12,14,16 mm
Numbers of column longitudinal reinforcements (*n*)	8-30
Spacing of the transverse reinforcement (*m*)	10-20 cm
Type I IDOT bearings	37 models (Table 7)
Retainer size of type I IDOT bearings (Anchor bolt of retainer)	7 models (Table 8)
Fixed-bearing model	13 models (Table 9)

4.2 Objective function

The goal of the optimization problem is to minimize the cost of seismic resisting system of the bridge (including piers and fusing components). Material and construction costs of pier concrete, longitudinal and transverse reinforcements, costs of IDOT bearing, anchor bolt and lateral retainers in the penalized objective function are considered. So the construction cost (ψ) of substructure of quasi-isolated bridge can be expressed as:

$$\begin{aligned}\psi = {} & V_C C_C + C_S\,(W_{SL} + W_{ST}) + \\ & 15(C_{IDOT1} + 2C_{Retainer}) + \\ & 5(C_{Fixed}) + \text{Penalty function}\end{aligned} \tag{1}$$

where, V_C is the volume of concrete in the designed pier column, C_C is the construction cost per volume of concrete (including material and labor cost), W_{SL} and W_{ST} are the weights of the designed longitudinal reinforcements and transverse reinforcements, respectively, and C_S is the construction cost per weight of reinforcement (including material and labor cost).

Regarding the quasi-isolation system configuration used in this parametric study, low-profile fixed bearings are installed at the second intermediate pier (Pier 2), while Type I elastomeric expansion bearings are used at the other pier and abutment locations. Each pier included five bearing that are installed on pier caps. As a result, generally there are 20 bearing for 2 piers and 2 abutments. (15 IDOT 1 elastomeric and 5 fixed bearing). C_{IDOT1} is the construction cost per each TypeI IDOT bearing (only for top plate, rubber layers and Steel shims-without retainer), $C_{Retainer}$ is the construction cost per each retainer, C_{Fixed} is the construction cost per each fixed bearing (including the anchor bolts). The unit costs of different materials are presented in Table 5.

Table 5: Unit costs of individual materials and bearing components

Item	Unit	Unit cost
C_C	per m^3	\$ 105
C_S	per ton	\$ 1200
C_{IDOT1}	per each	Table 7
C_{Fixed}	per each	Table 9
$C_{Retainer}$	per each	Table 8

4.3 Constant parameters

The constant design parameters are tabulated in Table 6.

Table 6: Constant design parameters

Parameter	Value
Span length (L)	25 m
Deck width (W)	11 m
Deck concrete girders Height	1 m
Concrete slab thickness	20 cm
Number of concrete girders	5

Distance between girders	1 m
Number of piers columns	3
Column Height	8 m
Pier Caps length	11.5 m
Depth of Pier Caps	1 m
Yield strength of reinforcement steel ($\boldsymbol{f_y}$)	400MPa
Unit weight of concrete	2400 kg/m^3
Unit weight of Steel	7850 kg/m^3
Concrete strength (MPa) $\boldsymbol{f_c'}$	35Mpa
Concrete tensile capacity	$f_t = 0.12 f_c'$
Modulus of elasticity of concrete	$4730\sqrt{f_c'}$ MPa
Modulus of elasticity of reinforcement steel	2e5MPa
Confined-to-unconfined concrete strength ratio	1.25
Live loads	HS20-44 (Truck and lane load)
Design traffic lane width	3.65 m
Thickness of asphalt wearing surface	8 cm
Unit weight of asphalt wearing surface	1730 kg/m^3
Site Class	Rock site "B"
Foundations type	fixed
Shear modulus of bearings	585 KPa
coefficient of friction values; $\boldsymbol{\mu_{SI}}$, $\boldsymbol{\mu_K}$, $\boldsymbol{\mu_{SP}}$ (fixed bearing)	0.31, 0.30 ,0.305
$\boldsymbol{\mu_{SI}}$, $\boldsymbol{\mu_K}$, $\boldsymbol{\mu_{SP}}$ (Type I IDOT bearing)	0.6 , 0.45 , 0.5
Shear Modulus(G)for Type I Bearings and Fixed Bearing	585 MPa
plastic hinge length , $\mathbf{l_p}$	$l_p = 0.05\,L + 0.1\,f_y d_b/\sqrt{f_c'}$

4.4 Constraints

Explicit and implicit constraints are imposed as lower and upper bounds on design variables based on geometrical restraints, construction limitations, and code requirements.

4.4.1 IDOT elastomeric bearing constraints

Type I IDOT bearings and fixed bearing are used for the prototype bridge, designed based on recommendations from the IDOT bridge manual. A number of feasible bearings that can be used in an optimal design (according to the percentage of dead and live load), is provided in Table 7. Provided in this table are geometric information including T_p, thickness of each rubber layer (cm), N_p, Number of rubber layers, ERT, total effective rubber thickness, N_s, number of steel shims, T_s, thickness of each steel shim, together with stiffness and estimated construction cost for common IDOT Type I bearings. Construction cost is based on General Contractors Price List–Western Region (2017) and reference [30]. Stiffness of each elastomeric bearing has been calculated as the shear modulus of the elastomer multiplied by the plan area of the bearing divided by the h_{rt} (ERT). A shear modulus of 585 KPa was used based on experimental results [29].

Table 7: Specifications for Type I IDOT bearings

Bearing type / Model number		Plan area ($cm \times cm$)	T_p	N_p	T_s	N_s	ERT	Stiffness (KN/m)	E. Construction cost
6-a	1	15×25	1.3	3	0.45	2	2.4	914.025	$ 555
6-b	2	15×25	1.3	5	0.45	4	4	548.45	$ 675
6-c	3	15×25	1.3	6	0.45	5	4.8	457.03	$ 735
7-a	4	18×30	0.95	3	0.85	2	2.8	1128.214	$ 750
7-b	5	18×30	0.95	4	0.85	3	3.8	831.315	$ 825
7-c	6	18×30	0.95	5	0.85	4	4.8	658.15	$ 900
9-a	7	23×30	0.95	5	0.85	4	4.8	840.93	$ 1050
9-b	8	23×30	0.95	7	0.85	6	6.7	602.462	$ 1192
9-c	9	23×30	0.95	8	0.85	7	7.6	531.11	$ 1260
10-a	10	25×35	1.8	5	0.45	4	5.5	930.681	$ 1287
10-b	11	25×35	1.8	6	0.45	5	6.7	763.992	$ 1377
10-c	12	25×35	1.8	7	0.45	6	7.7	664.77	$ 1452
10-d	13	25×35	1.8	8	0.45	7	8.9	575.140	$ 1542
11-a	14	28×40	0.3	4	0.45	3	5.1	1284.70	$ 1502
11-b	15	28×40	0.3	5	0.45	4	6.35	1031.81	$ 1596
11-c	16	28×40	0.3	6	0.45	5	7.7	850.90	$ 1697
11-d	17	28×40	0.3	7	0.45	6	8.9	736.17	$ 1787
12-a	18	30×45	2.3	3	0.8	2	4.3	1836.62	$ 1672
12-b	19	30×45	2.3	4	0.8	3	5.8	1361.63	$ 1785
12-c	20	30×45	2.3	5	0.8	4	7.2	1096.85	$ 1890
12-d	21	30×45	2.3	6	0.8	5	8.9	887.35	$ 2017
12-e	22	30×45	2.3	7	0.8	6	10	789.75	$ 2100
13-a	23	33×50	1.4	3	0.8	2	4.8	2010.75	$ 2010
13-b	24	33×50	1.4	4	0.8	3	6.35	1520.074	$ 2126
13-c	25	33×50	1.4	5	0.8	4	7.9	1221.83	$ 2242
13-d	26	33×50	1.4	6	0.8	5	9.6	1005.475	$ 2370
13-e	27	33×50	1.4	7	0.8	6	11.2	861.83	$ 2490
14-a	28	35×55	2.8	3	0.8	2	5.3	1930.5	$ 2227
14-b	29	35×55	2.8	4	0.8	3	7	1608.75	$ 2450
14-c	30	35×55	2.8	5	0.8	4	8.7	14076.56	$ 1985
14-d	31	35×55	2.8	6	0.8	5	10.5	1072.5	$ 2712
14-e	32	35×55	2.8	7	0.8	6	12.2	923.053	$ 2840
15-a	33	38×60	0.85	3	0.8	2	5.7	2340	$ 2707
15-b	34	38×60	0.85	4	0.8	3	7.62	1750.39	$ 2851
15-c	35	38×60	0.85	5	0.8	4	9.5	1404	$ 2992
15-d	36	38×60	0.85	6	0.8	5	11.5	1159.8	$ 3142
15-e	37	38×60	0.85	7	0.8	6	13.4	995.37	$ 3285

Notes:

1. The total effective rubber thickness is defined as the summation of the individual layers of rubber including the top and bottom layer.

2. (T_p = Thickness of each rubber layers (cm), N_p = Number of rubber layers, ERT = Total effective rubber thickness, N_s = Number of steel shims, T_s = Thickness of each steel shims)

4.4.2 L– shaped steel retainers design constraints

Anchor bolt diameters used in side retainers can be selected based on design recommendations from the IDOT Bridge manual. These include 16, 19, 25 and 32 mm for the abutments and 32, 38, 50, 64 mm for the piers. The ultimate capacity (P_{ult}) of each retainer assembly including two anchor bolts are calculated using equation (2), based on the threaded anchor bolt area and ultimate material strength, assuming a tensile failure condition.

$$P_{ult} = \varphi 0.8 A_{bolt} F_u \quad , \varphi = 1, \qquad F_u = 248 \text{ (MPa)} \tag{2}$$

Values of P_{ult} for different retainer sizes are presented in Table 8. The component total costs are also presented which are calculated based on the construction cost (C. Cost) per weight of anchor bolts and L-shaped retainer.

Table 8: Estimated capacities of retainers for IDOT type I bearing

Model number	**1**	**2**	**3**	**4**	**5**	**6**	**7**
Bolt Diameter (mm)	16	19	25	32	38	50	64
$A_{bolt}(mm^2)$	192	228	485	792	962	1756	3075
P_{ult}, **estimated** (**KN**)	118	140	184	236	280	368	472
C. Cost (2 bolts)	$22	$25	$35	$45	$55	$70	$85

4.4.3 Fixed-bearing design constraints

Table 9 presents possible combinations of anchor bolt and pintle sizes to determine the ultimate rupture capacity of fixed-bearing. The pintles are limited to a minimum diameter of 32 mm (1.25 in). The minimum pintle size specification typically results in bearings where the anchor bolts are smaller than the pintles and this is expected to cause the anchor bolts to be the more critical component that will fail first in an earthquake.

The fixed-bearing total cost is calculated based on construction cost per weight of anchor bolts, pintles and top and bottom steel plates. In general, the construction cost of fixed bearing is far less than IDOT elastomeric bearings.

Table 9: Ultimate capacity and construction costs of fixed-bearings

Fixed-bearing model	**Pintle size used in model**	**Bolt size used in model**	**Total ultimate capacity(KN)**	**E.C. Cost**
Model32/19	32	19	374	$ 155
Model32/25	32	25	529	$ 170
Model38/19	38	19	424	$ 170
Model38/25	38	25	529	$ 180
Model38/32	38	32	765	$ 195
Model50/19	50	19	659	$ 190
Model50/25	50	25	814	$ 205
Model50/32	50	32	1000	$ 220
Model50/38	50	38	1103	$ 230
Model64/19	64	19	1053	$ 225
Model64/25	64	25	1208	$ 180
Model64/32	64	32	1394	$ 195
Model64/38	64	38	1497	$ 205

4.4.4 Cross-sectional area of column constraints

Minimum column diameter is considered to be 80 cm due to construction limits. Based on the seismic design code for an RC structure (ACI Committee 318-05), the ratio of the cross-sectional area of the longitudinal reinforcement to the gross cross-sectional area of the RC section should be between 0.01 and 0.06. Moreover, based on ACI 318-05, the volumetric ratio ρ_s of transverse reinforcement shall satisfy

$$\rho_s \geq 0.45\left(\frac{A_g}{A_c} - 1\right)\frac{f'_c}{f_{yh}} \tag{3}$$

where A_g is the gross cross-sectional area of the column; A_c is the cross-sectional area of the column core measured out to out of transverse reinforcement;

4.5 Performance objectives

Performance objectives are groups of combined earthquake and performance levels. The Essential/Hazardous (E/H) performance objective is defined as a combination of Operational performance in the expected (design) earthquake and Life Safety performance in Maximum Considered Earthquake (MCE). The expected or design earthquake is considered to have a return period of 1,000 years, and the 'rare' earthquake is the one with 2,500 years return period. For a bridge meeting operational performance level, damage sustained is moderate and full service for emergency vehicles should be available after inspection. Bridge should be reparable subject to limited restrictions on traffic flow. A bridge meeting life-safety performance level is expected to have sustained significant damage during an earthquake and service is significantly disrupted, but life safety is assured. The two-level selected performance objective for prototype quasi-isolated bridge is presented in Table 10, specifying the expected damage levels. In this paper, lateral drift in pier columns is used as the engineering demand parameter for correlation with performance levels and damage states. For each performance level, the corresponding drift limits and ductility demands as recommended by [31, 32] are tabulated in Table 10.

Table 10: Performance objective and damage levels

Earthquake level	Probability of Exceedance in 75 Years (Return Period)	Performance level	Expected damage	Drift (Piers)	Ductility (Pier members)
Design level	7 %(1000 year)	Operational	Moderate	0.005	2.0
MCE level	3 % (2500 Year)	Life Safety	Significant	0.015	6.0

4.6 Structural modeling

The total length of the bridge is 75 m with 3 spans of 25 m. The bridge deck has 11 meters width and 20 cm thick concrete slab on five steel girders with 1m Height, located 2.3 m apart. All superstructure components were modeled with linear elastic elements because the quasi-isolated ERS concept features an essentially elastic superstructure

Substructure included multi-column piers with 3 concrete columns (8 m high) and a pier

cap with 11.5 m length and 1 m depth. In Csi Bridge [33], piers can be modeled using beam-column elements with fiber sections in the plastic hinge zones to capture material nonlinearities in the concrete and steel reinforcement. The multi-column piers can experience nonlinear phenomena (such as cracking and flexural yielding) when subjected to high lateral loads (Fig. 3.a). Thus, the distributed plasticity force-based beam-column element developed by Scott and Fenves [34] was used since it is capable of capturing the large curvature that could occur in the plastic hinge region of a concrete column. The plastic hinge length is defined as $l_p = 0.05\,L + 0.1\,f_y d_b/\sqrt{f'_c}$ (MPa), where L is the distance from the critical section to the point of contra-flexure, f_y is the longitudinal rebar yield strength, d_b is the diameter of that rebar, and f'_c is the concrete compressive strength (Fig. 3.b). A fiber section was used to model the nonlinear behavior in the plastic hinge regions of the column piers (Fig. 3.c). Concrete properties were defined as follows: a confined-to-unconfined concrete strength ratio of 1.25, concrete tensile capacity $f_t = 0.12f'_c$ and concrete modulus of elasticity $E_c = 4730\sqrt{f'_c}$.

Elastomeric bearings are modeled as link elements and the force-displacement relations from monotonic longitudinal loading of Type I & II bearings of experimental results from Steelman et al. [19] are used to simulate their stick–slip friction behavior (see Fig. 4 for an example). This nonlinear model represents the initial static breakoff coefficient (μ_{SI}), the kinetic coefficient (μ_k), and the post-slip breakoff (μ_{sp}) sometimes observed when the sliding direction reversed. For numerical modeling of retainers, the simplified force-displacement model shown in Fig. 5 is used. This model captures the basic observed behavior entirely through elasto-plastic response of the anchor bolt followed by failure at a user-defined ultimate displacement [17]. Fixed bearing are also modeled as links with total fuse capacity including both "friction force" from the elastomer and rupture capacity of the anchor bolts and pintles [35]. As noted in section 3, based on the experimental results, coefficient of friction values, μ_{SI}= 0.6, μ_K= 0.4, and μ_{SP}= 0.6 were used for the fixed bearings.

Also foundations were modeled as fixed, representing a rock bed. The site class is considered to be Site Class B based on the “Rock site” properties.

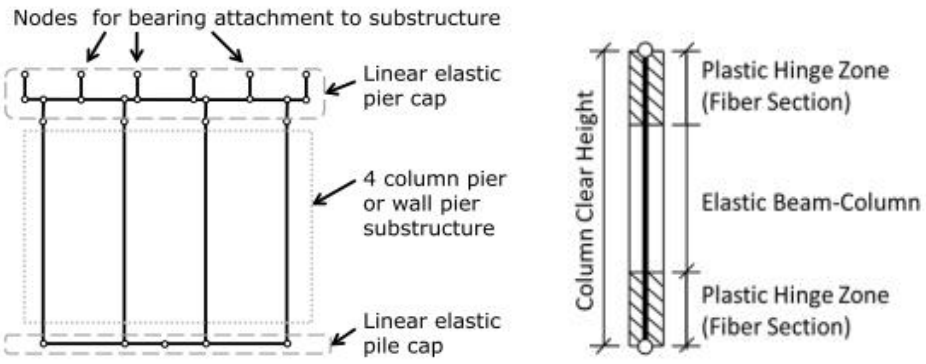

(a) Substructure schematic (b) Element and curvature distribution

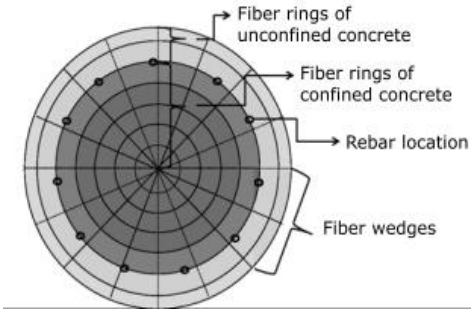

(c) Fiber sections used at hinge locations

Figure 3. Substructure details [17]

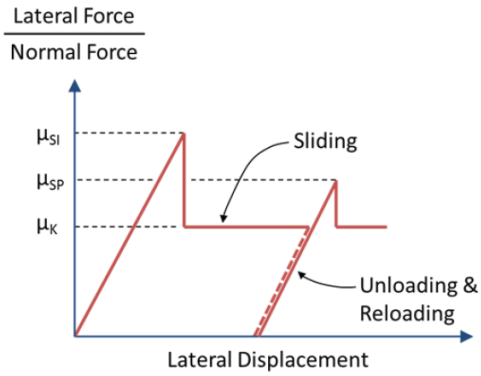

Figure 4. Force-Displacement model for IDOT Type I sliding bearing

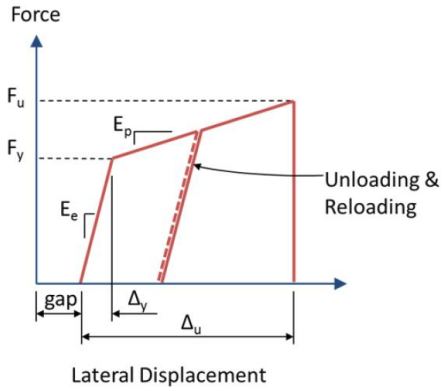

Figure 5. Force-Displacement model for retainers

4.7 Analysis and design method

The PBSD framework is based on DBD (Displacement based Design) method which is incorporated into AASHTO *Guide Specifications for LRFD Seismic Bridge Design*. DBD method is the most promising seismic design method under PBSD framework, since it uses target displacement to initiate a design. The target displacement is a good measurement to identify structural performance. In DBD, the bridge designer simply proposes a lateral load system and corresponding element strengths, and then checks to ensure that the displacement demand is less than the displacement capacity at each pier.

4.7.1 Seismic input

Seismic input is provided as the AASHTO seismic response spectra. The USGS web site [36] is used to obtain seismic hazard data for two hazard levels namely a design level earthquake (DBE) and a maximum considered earthquake (MCE) with 1000-yr and 2500-yr return periods, respectively. Spectral response acceleration parameters are obtained for a site class B (rock site). These parameters namely the design level spectral parameters for short period, S_{DS}, and 1s period, S_{D1}, are calculated as 0.972 and 0.625, respectively and the corresponding parameters at maximum considered earthquake i.e. S_{MS} and S_{M1} are obtained as 1.43 and 0.87, respectively. MCE & Design Response Spectra are shown in Fig. 6.

4.7.2 Capacity /Demand analysis of the structure

A two-step approach is used to analyze the bridge structure subject to intended seismic input. A linear dynamic modal response spectrum analysis is performed to obtain seismic displacement demands on the entire bridge structure. Adequate number of modes are included in the modal analysis to ensure that the total mass participation ratio is not less than 90 percent. Dynamic loads are applied along two separate longitudinal and transverse directions. Another load case is considered to account for Directional Combination of response spectrum loads using the 100/30 percent rule in each of the major directions.

Full 3D pushover analyses are performed to evaluate the displacement capacity of the structure. Each pier is analyzed in a transverse and longitudinal direction local to that pier, taking into account the superstructure and bearings at the subject pier. For each pushover case, the support bearings of the subject pier are kept and all other support bearings are changed to rollers. Transverse loads are applied according to load patterns proportional to mass distribution of the structure. The structure is pushed to the target displacement obtained from the multi-mode spectral analysis in the previous step. Capacity of each pier is evaluated at the target displacement considering the corresponding limits on demand parameters (drift and ductility of each column). All bearing retainers are meant to break off and permit bearing sliding during both earthquake hazard levels. Fixed bearing are also intended to fuse. However, seat widths are controlled to ensure that unseating of superstructure girders on piers and abutments does not occur.

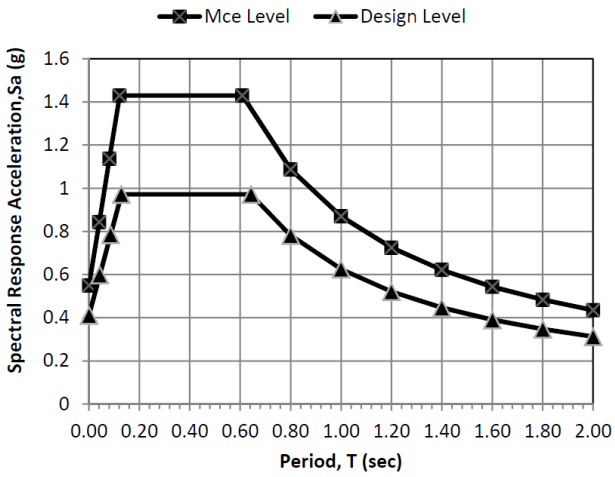

Figure 6. MCE & design response spectrum

4.8 Solution of optimal design problem

The optimal design problem for piers and bearings of a quasi-isolated bridge is highly nonlinear due to nonlinearity of cost function and constrains. Furthermore, the inter-dependence between analysis results and design variables increases the nonlinearity of the problem. It is well-known that the solution of large nonlinear optimization problems using mathematical programming methods becomes inefficient due to a large number of gradient calculations. Therefore, an extensive research effort has been devoted to developing powerful algorithms in order to find the global optimum in an affordable time without being

entrapped in local optima. Meta-heuristic optimization algorithms [37, 38] such as Genetic algorithms (GA) [39], Particle swarm optimization (PSO) [40], Ant colony optimization (ACO) [41], Big bang-big crunch (BB-BC) [42], Charged system search (CSS) [43], Ray optimization (RO) [44], Dolphin echolocation (DE) [45], Colliding Bodies Optimization (CBO) [46], are now well established and successfully applied to different structural optimization problems. The CBO algorithm proposed by Kaveh and Mahdavi [46] is a population-based algorithm which takes its inspiration from the physic laws of conservation of momentum and energy in physical systems encompassing colliding bodies. A modified version of this algorithm denoted by MCBO, is recently applied to the optimization of post-tensioned concrete bridge superstructures [47] and tunnel support linings [48]. In this paper, the MCBO is adopted for performance-based seismic design of quasi-isolated bridge system, due to its superior performance and ease of implementation. An outline of the implementation is presented in Fig. 7. One can refer to the above-mentioned articles for details of the algorithm.

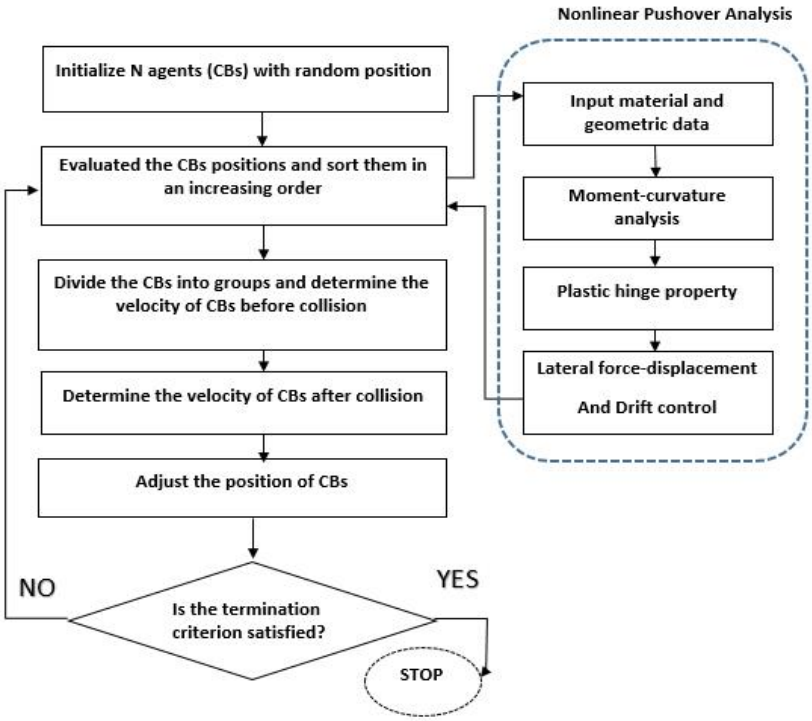

Figure 7. Flowchart of the proposed algorithm

5. RESULTS AND DISCUSSION

5.1 Optimum results

The prototype three - span bridge as discussed in section 4, is designed for Essential/Hazardous performance, using the proposed optimized framework. Earthquake resisting system consists of 20 bearings (15 IDOT + 5 Fixed) and two multi-column piers

(six concrete columns). The bearings are categorized in 3 groups (fixed-bearing for pier 2 , IDOT bearing for pier 1, and IDOT bearing for abutments 1 and 2). The algorithm is run 50 times and the minimum-cost design solution is presented in Table 11. In order to compare the performance of quasi-isolated bridge with a conventional system, another bridge model is created with monolithic pier-deck connections and common elastomeric bearing seats (without retainers) on abutments. The model is analyzed and designed using the same optimization algorithm. Table 11 also provides the total construction cost as well as the obtained design parameters for the conventional bridge. It is evident that a total saving of about 40 percent in construction cost may be achieved by taking account of quasi-isolation in seismic performance.

Table 11: The optimum design of Quasi-isolated and conventional bridges

Variable	Quasi-isolated bridge	Conventional bridge
Column diameter (mm)	850	1200
Arrangement of Longitudinal Reinforcements (n-$\mathbf{D_L}$)	32-D24	32-D28
Longitudinal Reinforcement Ratio, $\boldsymbol{\rho}$	1.84%	1.74%
Arrangement of Transverse reinforcement ($\boldsymbol{D_T}$-m)	D10@100 mm	D12@65 mm
Type of IDOT Bearing(for Abutments), 10B	IDOT 9-c	Gumba Type C (2)
Type of IDOT Bearing(for Pier1), 5 B	IDOT 12-b	------
Size of retainer for IDOT bearing, $\mathbf{D_{bolt-Retainer}}$ (mm)	Φ 25	------
Fixed-bearing model, 5 B	Model 32/19	------
Total Cost of substructure (Dollars)	57352.2	80293.2
Total Cost expressed as ratios	1.0	1.4

5.2 Discussion of performance of quasi-isolation system in optimal design

Longitudinal and transverse pushover curves are presented in Fig. 8 for the optimized quasi-isolated bridge design. The following key events in the longitudinal and transverse static pushover analysis are indicated in Fig. 8, with the associated progression of damage discussed below:

In longitudinal direction (Fig. 8,a), at the beginning (point A) the bridge experiences deformation and linear softening, then in part (B) with increases forces a friction-slip behavior occurs in the elastomeric bearings at intermediate pier (pier1, bearings that primarily carry girder and deck loads). In section B also expected, occurs Break-off of anchor bolts at low-profile fixed bearings, which were responsible for preventing movement under service loads. When it arrives at part (C), friction slip of the outside bearings at each abutment (bearings that carry parapet loads in addition to girder and deck loads) is observed. In the transverse direction, depending on the side retainers and the fuse mechanism, the interpretation conditions vary in the pushover curve; referring to Fig. 8,b, First, in part (A) due to low forces, it has a linear curve. Gradually, the push force is increased and the bearing top plate contacts with retainers at Abutment (the gap is closed). (B): Limited slip conditions occur in elastomeric bearings, while lateral retaining bolts are still resisting. At point (C), the bridge experiences a sudden drop in force due to the failure of the side retainers (first at the piers and then at the abutments). Between points B and C, the rotation of deck about Pier 1 occurs, with reverse movement of bearings at Abutments. Then, friction

slip in the remaining bearings is observed.

Fig. 9 presents transverse pushover curve for conventional bridge model without fusing components. The comparison between the curves indicates that, the Base-shear has significantly increased in the case of conventional bridge compared to the quasi-isolated system. In addition, the displacement demand decreases due to the added stiffness of the system.

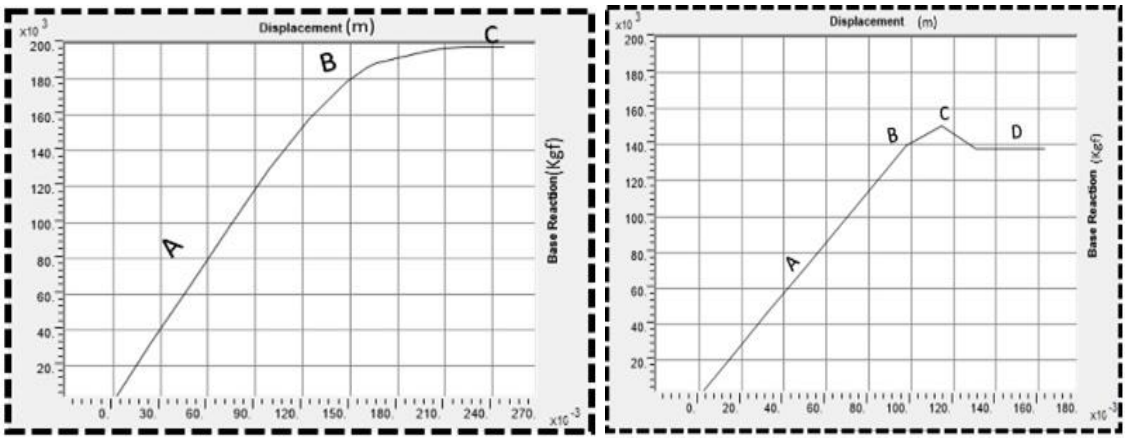

(a) Longitudinal direction (b) Transverse direction

Figure 8. Pushover curve for optimum quasi-isolated bridge

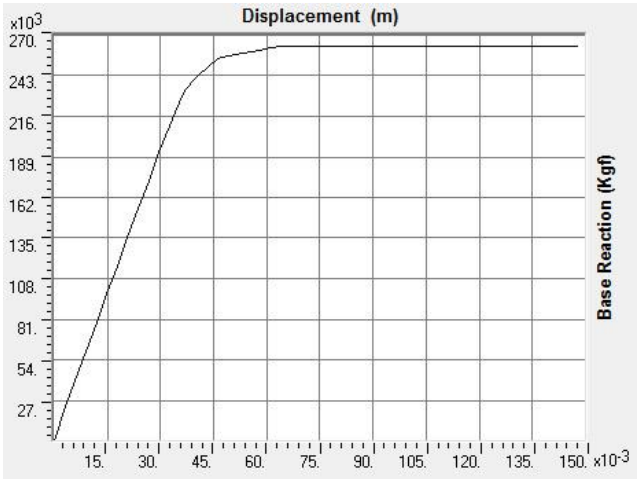

Figure 9. Transverse pushover curve for optimum conventional bridge

6. CONCLUSION

In this paper an optimization framework is presented for seismic design of bridges considering beneficial effects of fusing components on seismic performance of the quasi-isolated system. The proposed method is based on a two-step structural analysis consisting of a modal dynamic demand analysis and a nonlinear static capacity evaluation of the entire bridge structure. Based on results obtained from the implementation of the proposed design

optimization method, the following conclusions can be drawn:

1. The structural optimization algorithm provides a general framework for automated performance-based seismic design of quasi-isolated bridge system. The optimization algorithm replaces the conventional trial-and-error process to serve as a search engine capable of locating the most efficient design in terms of cost and performance.
2. Using the proposed framework, the potential for calibrating the fuse component capacities is exploited during the design process, such that a cost-effective design solution is obtained combining the fusing behavior of bearings and yielding mechanism of piers.
3. Computational models that address the effects of fusing components in seismic performance, lead to optimal designs that are considerably more favored in terms of minimum cost than those which do not account for quasi-isolation. Construction cost of a properly designed quasi-isolated system is reduced by 40 percent compared to that of an integral bridge without taking account of fusing mechanism.

REFERENCES

1. Gholizadeh S, Kamyab R, Dadashi H. Performance-based design optimization of steel moment frames, *Int J Optim Civil Eng* 2013; **3**: 327-43.
2. Fragiadakis M, Lagaros ND, Papadrakakis M. Performance-based multiobjective optimum design of steel structures considering life-cycle cost, *Struct Multidiscip Optim* 2006; **32**: 1-11.
3. Kaveh A, Azar BF, Hadidi A, Sorochi FR, Talatahari S. Performance-based seismic design of steel frames using ant colony optimization, *J Construct Steel Res* 2010; **66**: 566-74.
4. Kaveh A, Laknejadi K, Alinejad B. Performance-based multi-objective optimization of large steel structures, *Acta Mech* 2012; **223**: 355-69.
5. Fragiadakis M, Papadrakakis M. Performance-based optimum seismic design of reinforced concrete structures, *Earthq Eng Struct Dyn* 2008; **37**: 825-44.
6. Ataei H, Mamaghani M, Lui E. Proposed framework for the performance-based seismic design of highway bridges, *Struct Congr* 2017; 240-53.
7. Kowalsky MJ, Priestley M, Macrae GA. Displacement-based design of RC bridge columns in seismic regions, *Earthq Eng Struct Dynam* 1995; **24**: 1623-43.
8. Sung YC, Su CK. Fuzzy genetic optimization on performance-based seismic design of reinforced concrete bridge piers with single-column type, *Optimiz Eng* 2010; **11**: 471-96.
9. Association CS. Canadian highway bridge design code, Canadian Standards Association, 2014.
10. Marsh ML, Buckle IG, Kavazanjian Jr E. LRFD Seismic analysis and design of bridges reference manual, Federal Highway Administration (FHWA), 2014.
11. Mackie K, Stojadinović B. Performance-based seismic bridge design for damage and loss limit states, *Earthq Eng Struct Dyn* 2007; **36**: 1953-71.
12. Priestley M. Performance based seismic design, *Bullet New Zealand Soc Earthq Eng* 2000; **33**: 325-46.

13. Dawood HM, ElGawady M. Performance-based seismic design of unbonded precast post-tensioned concrete filled GFRP tube piers, *Composit Part B: Eng* 2013; **44**: 357-67.
14. Floren A, Mohammadi J. Performance-based design approach in seismic analysis of bridges, *J Bridge Eng* 2001; **6**: 37-45.
15. Marsh ML, Stringer SJ. Performance-based seismic bridge design, Washington, D.C, Transportation Research Board, 2013.
16. Tobias DH, Ralph E. Anderson, Chad E. Hodel, William M. Kramer, Riyad M. Wahab, Chaput ARJ. Overview of earthquake resisting system design and retrofit strategy for bridges in illinois, *Pract Period Struct Des Construct* 2088; **13**: 147-58.
17. Filipov ET, Fahnestock LA, Steelman JS, Hajjar JF, LaFave JM, Foutch DA. Evaluation of quasi-isolated seismic bridge behavior using nonlinear bearing models, *Eng Struct* 2013; **49**: 168-81.
18. Filipov ET, Revell JR, Fahnestock LA, LaFave JM, Hajjar JF, Foutch DA, et al. Seismic performance of highway bridges with fusing bearing components for quasi-isolation, *Earthq Eng Struct Dyn* 2013; **42**: 1375-94.
19. LaFave J, Fahnestock L, Foutch DA, Steelman J, Revell J, Filipov E, et al. Experimental investigation of the seismic response of bridge bearings, 2013.
20. Ghobarah A. Performance-based design in earthquake engineering: state of development, *Eng Struct* 2001; **23**: 878-84.
21. Poland CD, Hill J, Sharpe RL, Soulages J. Vision 2000: Performance based seismic engineering of buildings, *Structural Engineers Association of California (SEAOC)*, 1995.
22. Seismic Retrofitting Manual for Highway Structures: Part 1-Bridges. McLean, Va: Federal Highway Administration (FHWA), 2006.
23. Moehle J, Deierlein GG. A framework methodology for performance-based earthquake engineering, *13th World Conference on Earthquake Engineering*, Vancouver, BC, Canada 2004, pp. 3812-3814.
24. (AASHTO) AAoSHaTO. *Guide Specifications for LRFD Seismic Bridge Design*, 2nd ed, Washington, D.C, 2011.
25. (AASHTO) AAoSHaTO. *LRFD Bridge Design Specifications*, 6th ed, Washington, D.C, 2013.
26. (NCHRP) NCHRP. *Comprehensive Specification for the Seismic Design of Bridges*, ATC/MCEER Joint Venture, 2001.
27. Hose YD, Seible F. Performance evaluation database for concrete bridge components and systems under simulated seismic loads, *Pacific Earthq Eng Res Center* 1999.
28. (Caltrans) Office of Earthquake Engineering CDoT, Seismic Design Criteria, Version 1.7. Sacramento, CA, 2013.
29. Filipov E. Nonlinear seismic analysis of quasi-isolation systems for earthquake protection of bridges, University of Illinois at Urbana-Champaign, 2012.
30. Kovacevic M. Bridge Development Report Cost Estimating, scribd. com, 2016.
31. (NCHRP) NCHRP. *Performance-Based Seismic Bridge Design*, NCHRP Synthesis 440, Washington, DC, Transportation Research Board, 2013.
32. Lu Y, Gu X, Guan J. Probabilistic drift limits and performance evaluation of reinforced concrete columns, *J Struct Eng* 2005; **131**: 966-78.

33. Computers and Structures I. CSi bridge. Berkeley, California USA, 2011.
34. Scott MH, Fenves GL. Plastic hinge integration methods for force-based beam–column elements, *J Struct Eng* 2006; **132**: 244-52.
35. Steelman J, Filipov E, Fahnestock L, Revell J, LaFave J, Hajjar J, et al. Experimental behavior of steel fixed bearings and implications for seismic bridge response, *J Bridge Eng* 2013; **19**: A4014007.
36. http://earthquake.usgs.gov/hazards/apps/gis/.
37. Kaveh A. *Advances in Metaheuristic Algorithms for Optimal Design of Structures*, 2nd edition, Switzerland, Springer International Publishing, 2017.
38. Kaveh A. *Applications of Metaheuristic Optimization Algorithms in Civil Engineering*, Switzerland, Springer, 2017.
39. Goldberg DE, Holland JH. Genetic algorithms and machine learning, *Mach Learn* 1988; **3**: 95-9.
40. Eberhart RC, Kennedy J. A new optimizer using particle swarm theory, *Proceedings of the Sixth International Symposium on Micro Machine and Human Science* 1995, New York, NY, pp. 39-43.
41. Dorigo M, Maniezzo V, Colorni A. Ant system: optimization by a colony of cooperating agents, *IEEE Trans Syst Man Cybernet Part B* 1996; **26**: 29-41.
42. Erol OK, Eksin I. A new optimization method: big bang–big crunch, *Adv Eng Softw* 2006; **37**: 106-11.
43. Kaveh A, Talatahari S. A novel heuristic optimization method: charged system search, *Acta Mech* 2010; **213**: 267-89.
44. Kaveh A, Khayatazad M. A new meta-heuristic method: ray optimization, *Comput Struct* 2012; **112**: 283-94.
45. Kaveh A, Farhoudi N. A new optimization method: Dolphin echolocation, *Adv Eng Softw* 2013; **59**: 53-70.
46. Kaveh A, Mahdavi VR. Colliding bodies optimization: a novel meta-heuristic method, *Comput Struct* 2014; **139**: 18-27.
47. Kaveh A, Maniat M, Naeini MA. Cost optimum design of post-tensioned concrete bridges using a modified colliding bodies optimization algorithm, *Adv Eng Softw* 2016; **98**: 12-22.
48. Fazli H. Optimal design of tunnel support lining using mcbo algorithm, *Int J Optimiz Civil Eng* 2017; **7**: 339-54.